

cation¹⁵ of the 6^+ state at 8.79 MeV shift the center of interest away from the 4^+ level (the only one for which the agreement is better with $b/a=1.2$ than with $b/a=1.6$). As a matter of fact, it is reasonable to expect a better agreement for the $J=2$ and $J=8$ levels than for the $J=4$ and $J=6$ levels. In general, the mixing of configurations affects more strongly the higher J levels; in the ^{20}Ne case, however, there is no other $J=8$ wave function which could be mixed in within the $2s$, $1d$ shell. As for the $J=4$ level we found in a previous

¹⁵ J. A. Kuehner and J. D. Pearson, *Can. J. Phys.* **42**, 477 (1964).

work¹⁶ that configuration mixing brings it down by just about 1 MeV.

V. CONCLUSION

In the case of ^{22}Ne a calculation should now be made with a larger basis to find out if the configuration mixing adequately increases the spacing. As of now it certainly is too early to speculate about possible inversion of higher levels. (See question mark in Fig. 3.)

¹⁶ C. Abulaffio, *Nucl. Phys.* **81**, 71 (1966).

$^{19}\text{F}(d,n)^{20}\text{Ne}$ Reaction from 2.5 to 6.5 MeV*

A. W. BARROWS, JR.,† F. GABBARD, AND J. L. WEIL

Department of Physics and Astronomy, University of Kentucky, Lexington, Kentucky

(Received 8 May 1967)

The excitation functions of the ground- and first-excited-state neutron groups from the reaction $^{19}\text{F}(d,n)^{20}\text{Ne}$ have been measured at laboratory angles of 0° and 30° in the deuteron energy range of 2.5 to 6.5 MeV with energy steps of about 80 keV. In general, the fluctuations observed in the excitation functions are relatively small. The angular distributions of both neutron groups have also been measured at 3.062, 3.554, 3.851, 4.400, 4.938, 5.601, and 6.065 MeV. The ground-state group peaks strongly at 0° for energies above 4 MeV, while the first-excited-state group peaks at 30° for all energies, as expected from stripping theory for the known spins and parities of the levels of ^{20}Ne . The angular distributions measured at incident energies above 4.4 MeV have been fitted by distorted-wave Born approximation calculations. The spectroscopic factors determined in this way vary by approximately a factor of 2, becoming larger at the higher energies. The energy-averaged value of the spectroscopic factor for the ^{20}Ne ground state is found to be 0.40, and that for the first-excited state is 0.38. When compared with the predictions of various nuclear models, these values are found to be in agreement with the hypothesis that ^{20}Ne is a deformed nucleus.

1. INTRODUCTION

THE (d,n) reaction has been successfully used in nuclear spectroscopy for a number of years. The shapes of the angular distributions of the neutron groups can be used to fix the parities and give information about the spins of the levels of the residual nuclei.¹⁻³ The intensities of the neutron groups provide a measure of the spectroscopic factors of the corresponding levels,^{4,5} and these spectroscopic factors can be compared to the predictions of various nuclear models.

The primary purpose of this study of the $^{19}\text{F}(d,n)^{20}\text{Ne}$ reaction was to get reliable values of the spectroscopic factors for the ground- and first-excited states of ^{20}Ne from distorted-wave Born approximation (DWBA) fits

to the data. The neutron groups to the ground- and first-excited states of ^{20}Ne were easily resolved in this work. The second-excited-state group could also be identified in some of the neutron spectra, but no useful information concerning it could be extracted from the data.

The spins and parities for these three levels in ^{20}Ne are well known, and it has been suggested that they can be explained by a rotational model.⁶ On the assumption that ^{20}Ne is a deformed nucleus, spectroscopic factors have been calculated⁵ using Nilsson wave functions,⁷ and also using Bishop's modification⁸ of the Nilsson functions. Two shell-model calculations have been published in recent years which also give a rotational-type level structure for ^{20}Ne . The first of these, by Elliott,⁹ used the SU_3 classification of shell-

* This work was supported in part by the National Science Foundation.

† Present address: U. S. Army Nuclear Defense Laboratory, Edgewood Arsenal, Maryland.

¹ S. T. Butler, *Proc. Roy. Soc. (London)* **A208**, 559 (1951).

² A. B. Bhatia, K. Huang, R. Huby, and H. C. Newns, *Phil. Mag.* **43**, 485 (1952).

³ R. Huby, *Nature* **166**, 552 (1950).

⁴ R. Huby, *Progr. Nucl. Phys.* **3**, 177 (1953).

⁵ M. H. MacFarlane and J. B. French, *Rev. Mod. Phys.* **32**, 567 (1960).

⁶ G. Rakavy, *Nucl. Phys.* **4**, 375 (1957); A. E. Litherland, J. A. Kuehner, H. E. Gove, M. A. Clark, and E. Almqvist, in *Proceedings of the Rutherford Jubilee International Conference, Manchester, 1961*, edited by J. B. Birks (Heywood and Company Ltd., London, 1961), p. 811.

⁷ S. G. Nilsson, *Kgl. Danske Videnskab. Selskab, Mat.-Fys. Medd.* **29**, No. 16 (1955).

⁸ G. R. Bishop, *Nucl. Phys.* **14**, 376 (1959/60).

⁹ J. P. Elliott, *Proc. Roy. Soc. (London)* **A245**, 128 (1956); **A245**, 562 (1956); J. P. Elliott and M. Harvey, *ibid.* **A272**, 557 (1963).

model states. Spectroscopic factors for ^{20}Ne have been calculated using an extreme version of this model.¹⁰ More recently, Inoue *et al.*¹¹ have made a shell-model calculation for ^{20}Ne using a central residual interaction, and subsequently they have also published spectroscopic factors.¹² Our experimentally derived values of the spectroscopic factors for the ground- and first-excited states are compared to those calculated from all four of these models.

Cross-section measurements of the ground- and first-excited-state groups were made at deuteron energies from 2.5 to 6.5 MeV. The ground state Q -value for the $^{19}\text{F}(d,n)^{20}\text{Ne}$ reaction is 10.646 MeV, and hence the energies of the observed neutrons ranged from 11.5 to 17 MeV. Angular distributions were measured at 3.062, 3.554, 3.851, 4.400, 4.938, 5.601, and 6.065 MeV from 0° to 165° .

The reaction $^{19}\text{F}(d,n)^{20}\text{Ne}$ has been studied in recent years by many investigators, the most recent in the same energy region as the present work being that of Siemssen *et al.*¹³ Earlier work is reviewed in Ref. 13. Siemssen *et al.*¹³ used a time-of-flight spectrometer which resolved all neutron groups up to that corresponding to the 0^+ state of 6.75-MeV excitation. Butler curves were fitted to the angular distributions at 3.04-MeV bombarding energy for the neutron groups to the ground, first, second, and sixth excited states of ^{20}Ne . The fits were rather poor except for the group corresponding to the sixth (6.75-MeV) excited state. Data on this reaction taken between 1.0- and 2.5-MeV bombarding energy have recently been published by Warshaw *et al.*¹⁴ The reaction $^{19}\text{F}(^3\text{He},d)^{20}\text{Ne}$, which should yield the same information as that presently sought, has recently been reported on by Siemssen, Lee, and Cline.¹⁵

2. EXPERIMENTAL PROCEDURE

Equipment

Deuterons were accelerated by the University of Kentucky Van de Graaff accelerator. The beam was analyzed by a 90° magnet and focused on target by a pair of quadrupole magnets. The beam energy on target was defined to better than 0.1% in energy by the analyzing magnet whose field strength was measured with a NMR flux meter.

Fluorine targets were made by evaporating calcium fluoride onto 0.020-in.-thick by 1.25-in.-diameter tantalum disks. The target thickness was measured by observing the broadening of the 1.38-MeV γ -ray resonance

¹⁰ M. Harvey (private communication).

¹¹ T. Inoue, T. Sebe, H. Hagiwara, and A. Arima, Nucl. Phys. **59**, 1 (1964).

¹² T. Inoue, T. Sebe, H. Hagiwara, and A. Arima, Nucl. Phys. **85**, 184 (1966).

¹³ R. H. Siemssen, R. Felst, M. Cosack, and J. L. Weil, Nucl. Phys. **52**, 273 (1964).

¹⁴ S. I. Warshaw, D. A. Goldberg, and G. E. Owen, Phys. Rev. **151**, 834 (1966).

¹⁵ R. H. Siemssen, L. L. Lee, and Douglas Cline, Phys. Rev. **140**, B1258 (1965).

of the $^{19}\text{F}(p,\alpha\gamma)^{16}\text{O}$ reaction. The thickness of the target used in all measurements except the 4.938-MeV angular distribution was 0.43 ± 0.04 mg/cm². For the 4.938-MeV angular distribution, the target thickness was 1.55 ± 0.16 mg/cm². The Q -values of $\text{Ca}(d,n)\text{Sc}$ for the various calcium isotopes are all much smaller than those for fluorine, and hence there is no background of unwanted neutron groups.

The target assembly was electrically insulated from the beam tube and served as a Faraday cup to collect the beam current. The total charge accumulated during a run was measured with an electronic current integrator. A -300 -V secondary electron suppressor was used to ensure accurate beam-current measurement. The beam was collimated before entering this assembly with tantalum disks appropriately spaced along the beam tube and ranging in aperture from $\frac{5}{8}$ - to $\frac{1}{4}$ -in. diameter. The scintillation counter used for the detection of neutrons in this experiment was a 1 in. long by 1-in. diameter stilbene crystal. The detector was mounted on a rotating arm allowing measurements in the horizontal plane from 0° to 165° relative to the direction of the incident beam. The whole apparatus was centered over an eight-foot-deep neutron pit to give good open geometry.

The efficiency of the detector was calculated according to the formula of Swartz and Owen,¹⁶ $\eta(E_0, L) = n_H \sigma_H L F(a, L)$, where the notation is that of Ref. 16. The problem of multiple scattering as well as edge effects and end effects were neglected in the calculation of efficiencies. For a crystal as short as the one used, the multiple-scattering effects are less than 1% for neutron energies above 9 MeV. End and edge losses can be neglected because the dimensions of the crystal are large compared to the proton range (0.2 cm for 15-MeV protons) in stilbene.

Accumulation of Data

Angular distribution measurements were made from 0° to 165° in 15° steps except at small angles where the steps were 5° or 10° . An angular distribution was measured approximately every 500 keV from 3 to 6 MeV. Excitation functions were also measured at 0° and 30° with energy steps of approximately 80 keV. The energy resolution ranged from 60 keV at 3 MeV to 35 keV at 6 MeV bombarding energy and was determined by the target thickness.

Since the $^{19}\text{F}(d,n)^{20}\text{Ne}$ reaction is accompanied by a large number of gamma rays, it was necessary to discriminate between neutrons and γ -rays in the data-taking procedure. Pulse-shape discrimination (PSD) was used to eliminate the γ -ray pulses from the spectra in the manner described by Retz-Schmidt and Weil.¹⁷

¹⁶ C. D. Swartz and G. E. Owen, in *Fast Neutron Physics, Part I*, edited by J. B. Marion and J. L. Fowler (Interscience Publishers, Inc., New York, 1960), p. 211.

¹⁷ T. Retz-Schmidt and J. L. Weil, Phys. Rev. **119**, 1079 (1960).

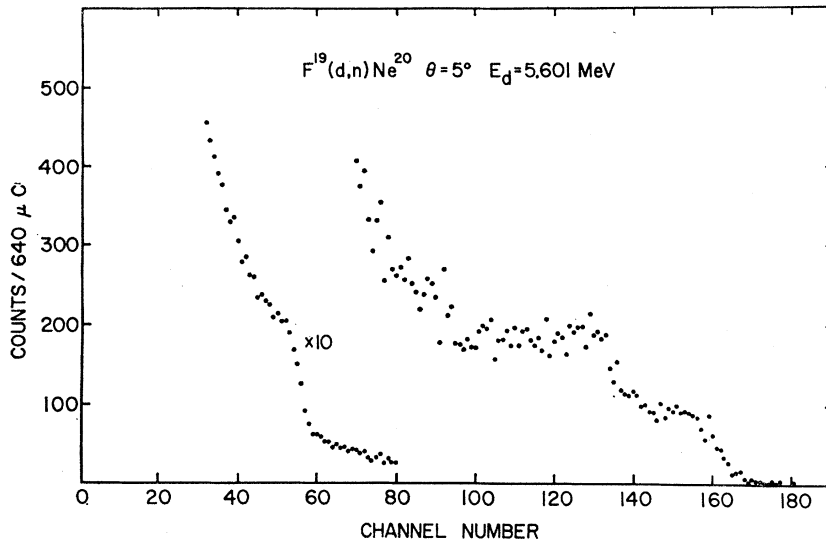


FIG. 1. Recoil proton spectrum in the stilbene crystal. $E_d=5.60$ MeV, $E_{n_0}=16.20$ MeV, and $E_{n_1}=14.62$ MeV. Plateaus due to the ground- and first-excited-state neutron groups can be seen.

The data taken were proton recoil spectra from the stilbene detector such as shown in Fig. 1. Pulses due to recoil protons were selected upon arrival at the multi-channel analyzer by requiring that the linear pulse from the detector be in coincidence with a gating pulse generated by the PSD circuit (Ref. 17). After proper focusing and beam alignment, the system was checked by observing the gated and ungated spectra for monoenergetic neutrons from the $T(d,n)^4He$ reaction to be

sure that the bias was not so high as to be discriminating against large numbers of neutron pulses.

Reduction of Data

The differential cross sections were calculated from the yields of the neutron groups using the formula,

$$d\sigma/d\omega = Y/\Omega n N \eta,$$

where Y is the yield extracted from the proton recoil

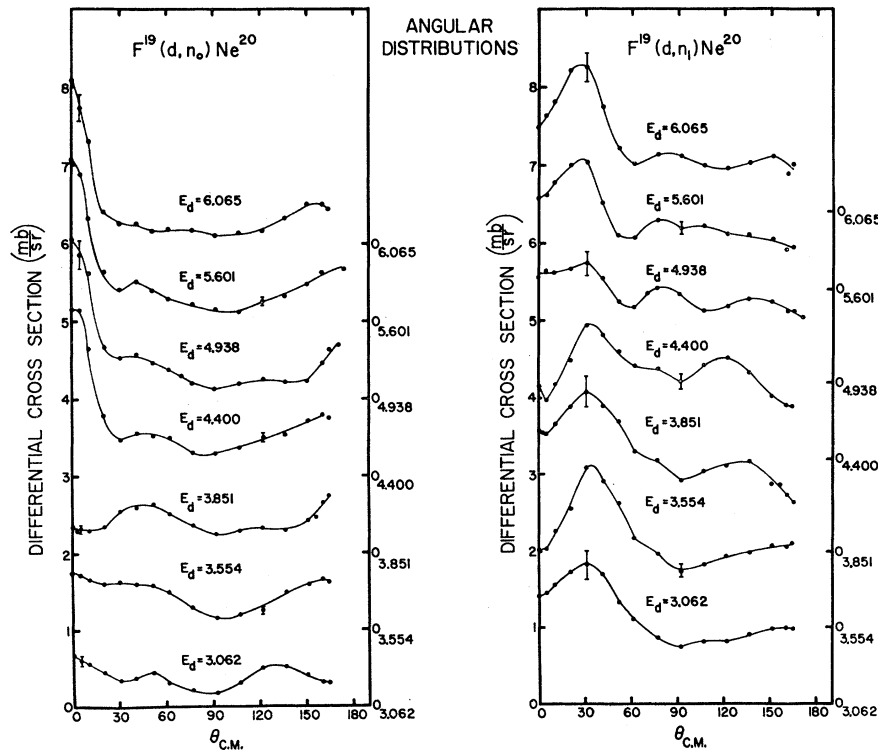


FIG. 2. The angular distributions at several bombarding energies of the neutron groups corresponding to the ground- and first-excited states of ^{20}Ne . The error in the absolute cross section is shown by error flags on a few typical data points.

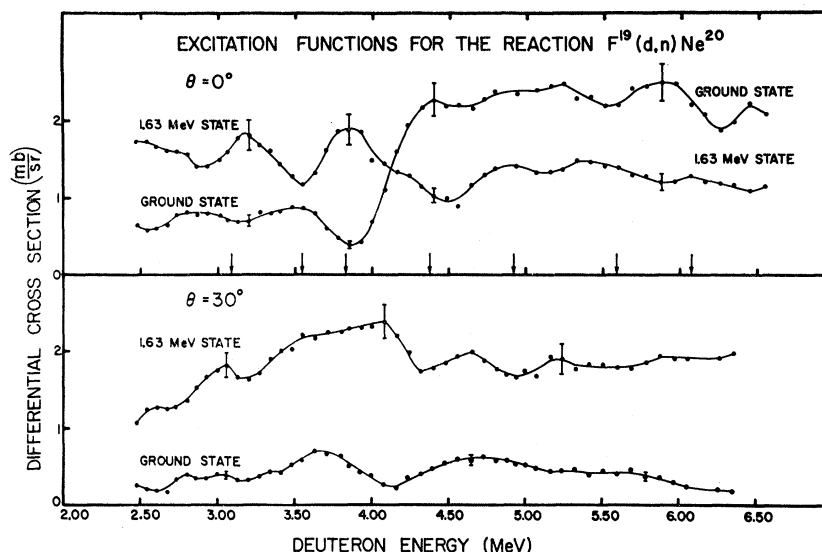


FIG. 3. The excitation functions of both neutron groups at 0° and 30° lab angle. The arrows show the energies at which the angular distributions were measured. The error in the absolute cross section is shown by the error flags on a few typical points.

spectrum, Ω is the solid angle subtended by the detector, n is the number of atoms per square centimeter in the target, N is the number of deuterons incident on the target, and η is the detector efficiency for counting neutrons. The methods for extracting the yields of the two neutron groups are given in Ref. 17 and by Din and Weil.¹⁸

Experimental Errors

The standard error assigned to the absolute cross sections was determined from the uncertainties in target thickness, statistics, data-reduction procedures, and integrated charge. The estimated errors from these sources are $\pm 10\%$, $\pm 3\%$, $\pm 5\%$, and $\pm 2\%$, respectively. When combined, they give a standard error of $\pm 12\%$ in the absolute cross sections and $\pm 6\%$ in the relative cross sections.

3. RESULTS

Angular Distributions and Excitation Functions

The angular distributions for the neutron groups to the ground- and first-excited states of ^{20}Ne are shown in Fig. 2. Below 4 MeV, the ground-state angular distributions vary rapidly with energy. Above 4 MeV, however, they all peak very strongly at 0° . This energy-independent character is indicative of a direct interaction stripping process with an $l_p=0$ for the spins and parities of the levels involved.¹⁹

For the first-excited-state group all the angular distributions peak around 30° . This is consistent with an $l_p=2$ orbital angular-momentum transfer which is also uniquely predicted.¹⁹ Other structure observed in the angular distributions seems to be peculiar to the par-

ticular bombarding energy and may indicate that reaction mechanisms other than stripping are also present.

The excitation curves are shown in Fig. 3. For the ground state at 0° , there is no significant structure except for the marked change in magnitude in the neighborhood of 4 MeV. The relatively smooth curve above 4 MeV is another indication of the direct interaction process. For the first-excited-state group at 0° there is definite structure at 3.2 and 3.8 MeV which cannot be explained by the direct interaction process, but the excitation curve is smooth above 4.8 MeV.

The 30° excitation function for the ground-state group has little structure except for a dip at 4.1 MeV. The first-excited-state group is also smooth with the exception of the slow rise up to 4 MeV and a small but sharp decrease in the cross section in the region of 4.2 MeV.

The relative smoothness of the excitation functions at high energies supports the validity of the comparison with stripping theory. The errors shown are the standard errors of the absolute cross sections, and the lines are only drawn to connect the data points.

Comparison of the present data with earlier published results can only be made at bombarding energies of 3.06 and 3.57 MeV. Our angular distributions agree with those of Siemssen *et al.*¹³ at 3.06 MeV in both absolute magnitude and shape to within the stated errors, except that we do not observe the narrow peak at 0° for the ground-state neutron group seen in the earlier experiment. The agreement is not so good at 3.57 MeV, where we find that our cross sections are about 2.5 times smaller than those measured by Benenson *et al.*²⁰ at 3.55 MeV. There is also considerable difference between the two experiments in the shape of the angular distributions.

¹⁸ G. U. Din and J. L. Weil, Nucl. Phys. 71, 641 (1965).

¹⁹ F. Ajzenberg-Selove and T. Lauritsen, Nucl. Phys. 11, 1 (1959).

²⁰ R. E. Benenson, H. Y. Chen, and L. J. Lidofsky, Phys. Rev. 122, 874 (1960).

DWBA Analysis

DWBA calculations were made using an automatic parameter-search program developed by Allison and McEllistrem²¹ and coded for the IBM 7040 at the University of Kentucky. The program adjusts the parameters of the optical-model potentials so as to minimize the deviation between experimental and theoretical cross sections. It can simultaneously fit the angular distributions of two different reactions. It is possible to require that any or all of the parameters be the same for the fits to both reactions. A complete description of the program is available at the University of Kentucky Department of Physics.

The complex optical-model potential used in this analysis made use of surface absorption and was of the form:

$$U(r) = U_c(r) - \frac{V}{1+e^x} - 4iW \frac{e^{x'}}{(1+e^{x'})^2},$$

where

$$x = (r-R)/a, \quad x' = (r-R')/a'$$

and $U_c(r)$ is the Coulomb potential based on a uniform charge of radius r_c .

$$U_c(r) = \frac{Ze^2}{2r_c^2} \left(3 - \frac{r^2}{r_c^2} \right), \quad r < r_c$$

$$= \frac{Ze^2}{r}, \quad r > r_c.$$

The value $r_c = 3.7$ F was used. Fits were attempted using volume absorption, but were considerably less satisfactory than with surface absorption.

Since no elastic scattering data were available for $d+^{19}\text{F}$ or $n+^{20}\text{Ne}$ in the energy range of these reported measurements, the following procedure was used to obtain optical-model parameters. The ground- and first-excited-state data were fitted at each bombarding energy by allowing the program to search on all optical-model potentials. These potentials were at first required to be the same for both reactions at a given energy. Several fits were obtained and one was chosen so that the deuteron real and imaginary potentials roughly agreed with values obtained by extrapolating the B set of potentials calculated by Perey.²² Using these deuteron potentials, the fits to the two reactions were improved by allowing the program to search on the neutron potentials. The neutron potentials arrived at seem to be quite reasonable when compared to the optical-model fits to the meager scattering data in this mass region.²³ As a final polish to the fits, the program searched on the diffusenesses which were required to

be the same for both final states. All calculations were made assuming a finite-range force and no spin-orbit potentials were included in any channel. Finite-range forces were included by using the local energy approximation (LEA)²⁴ in a zero-range code. A factor of 1.7 was applied to the zero-range results to correct them for the difference²⁵ between the Hulthén and the zero-range deuteron wave functions. Compound nucleus contributions were neglected. The optical-model parameters obtained in this way varied smoothly with bombarding energy.

It was most gratifying to find, after these calculations were completed, that the deuteron potential parameters thus obtained were in such good agreement with the results of Satchler's recent work²⁶ on $^{12}\text{C}(d,d)^{12}\text{C}$. However, it is interesting to note that in our case the deuteron real potential depth dropped with decreasing deuteron energy while for $^{12}\text{C}(d,d)^{12}\text{C}$ it increases.²⁶ Also, as was found by Satchler²⁶ for the case of elastic scattering, the shape of our angular distributions were strongly dependent on small changes in the parameters. However, the spectroscopic factors were rather insensitive to small parameter changes. The small diffuseness values in the present work at 4.400 and 4.938 MeV were found to be necessary to get a good fit to the first-excited state data between 60° and 110° . Anomalous values of a_d' were found necessary²⁶ for similar reasons in $^{12}\text{C}(d,d)^{12}\text{C}$.

The bound-state wave function was calculated using a Woods-Saxon potential by adjusting the depth so that the binding energy of a proton in ^{20}Ne was correct. Since this wave function, and hence the magnitude of the cross sections, is strongly dependent on the choice of parameters for this well, calculations were made varying the radius from 3.3 to 5.0 F. The peak cross sections for the two reactions changed by a factor of five between these two extremes and increased most rapidly when the radius became large. Of course, since the deduced experimental spectroscopic factors are inversely proportional to these calculated DWBA cross sections, they too are dependent on the radius of the bound state well. The uncertainty in the exact value to use for this radius causes uncertainty in the derived spectroscopic factors.²⁷ However, the ratio of spectroscopic factors for the ground state and first-excited state was found to vary less than 10% over a broad range of bound-state radius. The radius used in all calculations was 3.9 F.

²¹ J. F. G. Perey and D. Saxon, Phys. Letters **10**, 107 (1964); P. J. A. Buttle and L. J. B. Goldfarb, Proc. Phys. Soc. (London) **83**, 701 (1964); G. Bencze and J. Zimanyi, Phys. Letters **9**, 246 (1964).

²² R. H. Bassel, R. M. Drisko, and G. R. Satchler, Oak Ridge National Laboratory Report No. ORNL-3240, p. 28 (unpublished); G. R. Satchler, *Lectures in Theoretical Physics, 1965* (University of Colorado Press, Boulder, Colorado, 1965), p. 122; G. R. Satchler (private communication).

²³ G. R. Satchler, Nucl. Phys. **85**, 273 (1966).

²⁴ J. L. Allison and M. T. McEllistrem (to be published).
²⁵ C. M. Perey and F. G. Perey, Phys. Rev. **132**, 755 (1963).
²⁶ F. Bjorklund and S. Fernbach, Phys. Rev. **109**, 1295 (1958); B. Johansson, Nucl. Phys. **67**, 289 (1965); H. F. Lutz, J. B. Mason, and M. D. Karvelis, *ibid.* **47**, 521 (1963).

²⁷ G. R. Satchler, Argonne National Laboratory Report No. ANL 6878, II, (1964), p. 37 (unpublished).

Spectroscopic Factors

The "best" DWBA fits to the 6.065-, 5.601-, 4.938-, and 4.400-MeV data are shown in Figs. 4 and 5. The optical-model parameters for these fits are listed in Table I along with the experimentally determined spectroscopic factors. The following parameters were the same for all the fits: $R_d=3.60$ F, $R_d'=3.70$ F, $R_n=3.68$ F, $R_n'=4.00$ F, $r_c=3.70$ F, and for the bound state $R_b=3.90$ F, $a_b=0.73$ F. The bound-state well depth was 61.5 MeV for the ground state and 57.3 MeV for the first-excited state.

Good fits at the three lowest energies could not be found. This is reasonable in light of the rapidly changing

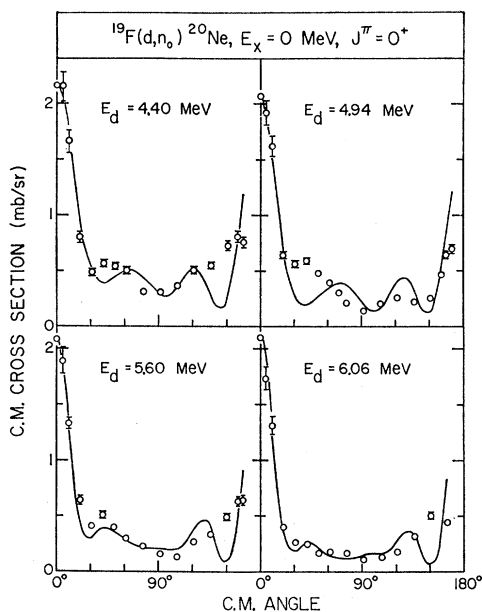


FIG. 4. Best DWBA fits obtained for the ground-state angular distributions at the four highest bombarding energies. No reasonable fits could be found for the lower energies. The optical-model parameters and spectroscopic factors corresponding to these fits are given in Table I. The relative errors are shown by the flags when they are larger than the size of the data points.

shapes of the angular distributions that are observed between 1.0- and 3.3-MeV bombarding energy.^{13,14}

Comparison with Theory

As mentioned in the Introduction there are four nuclear models to which comparison can be made; two versions of the rotational model and two versions of the shell model. Theoretical spectroscopic factors have been calculated for the former using Nilsson wave functions⁷ as outlined in MacFarlane and French⁵ and also using the modified Nilsson wave functions of Bishop.⁸ Bishop⁸ has added the term μl^2 to the Nilsson Hamiltonian for low- A nuclei and has obtained wave functions that correspond to a better fit to the level structures of

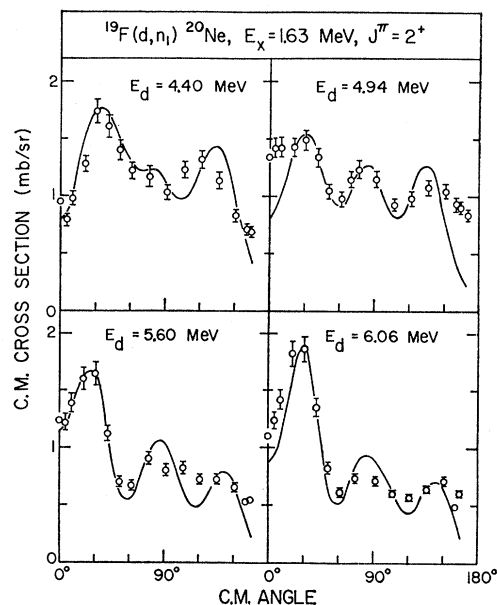


FIG. 5. Best DWBA fits obtained for the first-excited-state angular distributions at the four highest bombarding energies. No reasonable fits could be found for the lower energies. The optical-model parameters and spectroscopic factors corresponding to these fits are given in Table I. The relative errors are shown by the flags when they are larger than the size of the data points.

nuclei with $A \leq 25$. A value $\mu = 0.167$ has been assumed in calculating the spectroscopic factors. Results of these calculations are given in Table II.

The published spectroscopic factors of Harvey^{10,15} and Inoue *et al.*,¹² whose calculations use an extreme version of the SU_3 shell model and a more conventional shell model, respectively, are also given in Table II. Harvey's SU_3 shell-model calculation assumed that the quadrupole-quadrupole force dominates the residual interaction and exchange forces are such as to favor states

TABLE I. Optical-model parameters and experimental spectroscopic factors from best DWBA fits.

E_d (MeV)	4.400	4.938	5.601	6.065
V_d (MeV)	99.0	100.3	106.0	109.0
W_d (MeV)	11.1	13.7	15.6	14.7
a_d (F)	0.53	0.58	0.70	0.70
a_d' (F)	0.43	0.64	0.60	0.60
Ground state:				
V_n (MeV)	45.1	47.6	52.4	52.4
W_n (MeV)	1.3	2.0	2.6	2.6
Excited state:				
V_n (MeV)	49.0	54.5	58.4	54.6
W_n (MeV)	4.0	4.5	5.2	4.9
a_n (F) ^a	0.73	0.76	1.01	1.01
a_n' (F) ^a	0.34	0.20	0.64	0.64
S_0	0.31	0.34	0.51	0.47
S_1	0.22	0.25	0.37	0.53

^a These diffuseness parameters were used for both ground- and first-excited states.

TABLE II. Experimental and theoretical spectroscopic factors for ^{20}Ne .

E_x (MeV)	J^π	U. Ky. (d,n) $\langle S_{\text{exp}} \rangle$	Calvert <i>et al.</i> (d,n) S_{exp}	Siemssen <i>et al.</i> ($^3\text{He},d$) S_{exp}	Nilsson S_{th}			Bishop S_{th}			Harvey SU_3 S_{th}	Inoue <i>et al.</i> S_{th}
					$\eta = +2$	$+4$	$+6$	$+2$	$+4$	$+6$		
	0 ⁺	0.40	0.65	0.31	0.31	0.49	0.57	0.22	0.41	0.50	0.43	0.49
	2 ⁺	0.38	0.70	0.63	0.34	0.30	0.29	0.36	0.32	0.30	0.24	0.38
$S(0^+)/S(2^+)$		1.05	0.93	0.49	0.91	1.63	1.97	0.61	1.28	1.67	1.79	1.29

of maximum orbital symmetry. The structure of the ^{19}F ground state was assumed to have the SU_3 classification⁹ $(\lambda, \mu) = (6, 0)$ with $L=0$, $S=\frac{1}{2}$, and $J=\frac{1}{2}$. Making the assignment $(\lambda, \mu) = (8, 0)$ for the $K=0$ ground-state band in ^{20}Ne , the spectroscopic factors in Table II were obtained.

Also given in Table II for comparison with the model calculations are the energy averaged values of the spectroscopic factors as measured in this experiment. From Table I it can be seen that the measured spectroscopic factors for both the ground- and first-excited states vary with energy. This is not unexpected in light of the fluctuations observed in all the excitation functions. Because it is not possible to unambiguously interpret the measured spectroscopic factor variations and because DWBA is really an energy-averaged theory, it was felt that the most meaningful information would be attained from a simple energy average of the experimental spectroscopic factors for each level. The results of the $^{19}\text{F}(d,n)^{20}\text{Ne}$ experiment by Calvert *et al.*,²⁸ and the $^{19}\text{F}(^3\text{He},d)^{20}\text{Ne}$ experiment of Siemssen *et al.*,¹⁵ have also been included in Table II for comparison.

The energy averaged spectroscopic factors from the present experiment are seen to be in rough ($\sim 30\%$) quantitative agreement with all four nuclear models. This is not too surprising since all of the models represent a nonspherical nucleus and give about the same level structure. For the Nilsson and Bishop models the correct value of the deformation parameter would seem to be in the range $3 \leq \eta \leq 4$.

It was noted earlier that varying the radius of the bound state potential well changes the absolute magnitudes of the spectroscopic factors for the two levels, but not their ratio. Hence more reliance should be placed on this ratio, which is also given in Table II, than on the individual magnitudes. The experimental value of the ratio favors the Nilsson and Bishop models for $\eta \approx +3$. The ratio of Calvert *et al.*,²⁸ obtained for 9-MeV deuteron energy with plane-wave Born-approximation fits is in good agreement with this. The fact that the $(^3\text{He},d)$ ratio differs from the (d,n) ratio is not too surprising in view of the poor fit to the $(^3\text{He},d_0)$ angular

distribution. Both the ratio difference and the poor fit might be attributed to the fact that no search was made on the optical-model parameters in the DWBA fitting procedure.¹⁵

4. CONCLUSIONS

A consistent DWBA analysis has been made which gives good fits to the $^{19}\text{F}(d,n)^{20}\text{Ne}$ cross sections for two outgoing channels over the range of incident energy from 4.4 to 6.1 MeV. The fact that this analysis is made with reasonable distorting potentials which are very little different for the two channels supports the assumption that these are essentially direct proton transfer reactions. However, the detailed structure of the excitation functions and angular distributions indicates the presence of other reaction mechanisms, while the energy dependence of the measured spectroscopic factors indicates an incomplete analysis of these reactions. By energy averaging the spectroscopic factors, it is hoped that the effects of what we are ignoring in the analysis are at least partially cancelled out.

Assuming that the averaging is a valid procedure, the argument that ^{20}Ne is a deformed nucleus is in reasonable agreement with the results of this experiment. However, the energy variations of the spectroscopic factor determinations and the uncertainty in the scale of their absolute magnitude makes it impossible to choose definitely between the various theoretical representations of this deformation. There is some favoring of the Nilsson or Bishop wave functions with $\eta \approx +3$, while the SU_3 shell model appears to be least likely to correspond to these data.

ACKNOWLEDGMENTS

The authors are most grateful to Professor M. T. McEllistrem and Dr. J. L. Allison for the use of their DWBA program and especially to Professor McEllistrem for many long discussions concerning the interpretation of the results of the calculations. Many thanks are due the University of Kentucky Computing Center for providing computer time for the reduction and analysis of the data. Ronald Proffitt is thanked for his work in performing some of the DWBA fits.

²⁸ J. M. Calvert, A. A. Jaffe, and E. E. Maslin, Proc. Phys. Soc. (London) A68, 1017 (1955).